HHS Public Access

Author manuscript

Nat Neurosci. Author manuscript; available in PMC 2009 November 01.

Published in final edited form as:

Nat Neurosci. 2009 May ; 12(5): 611–617. doi:10.1038/nn.2291.

Oxidation of a potassium channel causes progressive sensory function loss during ageing

Shi-Qing Cai and **Federico Sesti**[§]

University of Medicine and Dentistry of New Jersey, Robert Wood Johnson Medical School, Department of Physiology and Biophysics, 683 Hoes Lane, Piscataway, NJ 08854, USA

Abstract

A central question is whether potassium (K^+) channels, which are key regulators of neuronal excitability, are targets of reactive oxygen species (ROS) and whether these interactions have a role in the mechanisms underlying neurodegeneration. Here, we show that oxidation of K^+ channel KVS-1 during ageing causes sensory function loss in *Caenorhabditis elegans*, and that protection of this channel from oxidation preserves neuronal function. Chemotaxis, a function controlled by KVS-1, was significantly impaired in worms exposed to oxidizing agents, but only moderately affected in worms harboring an oxidation-resistant KVS-1 mutant (C113S). In ageing C113S transgenic worms, the effects of free radical accumulation were significantly attenuated compared to wild type. Electrophysiological analyses showed that both ROS accumulation during ageing, or acute exposure to oxidizing agents, acted primarily to alter the excitability of the neurons that mediate chemotaxis. Together, these findings establish a pivotal role for ROS-mediated oxidation of voltage-gated K^+ channels in sensorial decline during ageing in invertebrates.

INTRODUCTION

Oxygen metabolism leads to the production of highly reactive molecules known as reactive oxygen species (ROS) which have important roles in the physiology and pathophysiology of the nervous system. With the passage of time, the redox environment of the neurons can be altered in favor of oxidation by an increased production of ROS or by a decreased activity of antioxidant defenses which include both enzymatic and non-enzymatic antioxidants. This condition, which is known as oxidative stress, is thought to represent a general contributing factor to ageing in biological systems 1. Uncontrolled ROS can cause considerable cellular damage by interacting with proteins, DNA and cell membranes 1. Thus, oxidative damage may not only contribute to the mechanisms leading to the progressive sensory and cognitive function loss which is part of the normal ageing process, but it has also been implicated in neurodegeneration characteristic of diseases such as Alzheimer's 2.

[§]address correspondence to: Federico Sesti, Ph.D., Tel: (732) 235 4032, Fax: (732) 235 5038, email sestife@UMDNJ.EDU.

Author contributions: S-Q. C. and F.S. designed research, performed research and analyzed data. F. S. wrote the manuscript.

Full Methods and any associated references are available in the online version of the paper (in supplemetary information)

K^+ channels are a fundamental class of integral membrane proteins which are essential to neuronal function and survival. It is possible that the interaction of ROS with K^+ channels may cause modifications of membrane currents and potentials thereby leading to neuronal dysfunction. In fact, many K^+ channels including voltage-gated (Kv) channels 3, 2-P domains channels 4, BK channels 5 and GIRK K^+ channels 6 can be modified by oxidizing agents *in vivo* and *in vitro*. However, with the exception of a few studies that suggest a potential role for oxidation of K^+ channels during neuronal hypoxia 7,8, the notion that modification of K^+ channels by ROS can be a mechanism of neurodegeneration has remained an intriguing but unproven hypothesis.

To address the fundamental question of whether K^+ channels can be physiological targets of ROS and whether these interactions may have a role in the mechanisms underlying age-related neurodegeneration, we employed the metazoan *Caenorhabditis elegans* since it is a well-established model to study biological processes related to ageing 9. In particular, the nervous system of the worm expresses KVS-1, a voltage-gated K^+ channel whose physiological characteristics—it plays a crucial role in the maintenance and sensitivity of the nervous system of the animal 10—make it a prime candidate to investigate the impact of oxidation of Kv channels on neuronal function.

Here, we show that modification of KVS-1 by endogenous ROS during ageing leads to sensorial decline and that protection of this channel from oxidation preserves neuronal function.

RESULTS

KVS-1 is susceptible to redox-modulation

In Fig. 1a are shown exemplar whole-cell KVS-1 currents that were elicited in CHO cells by voltage steps from -80 mV (holding voltage) to +120 mV in 20 mV increments. Five minutes exposure to the oxidizing agent chloramine-T (CHT) in the bath solution slowed inactivation of KVS-1 (Fig. 1a. $\tau = 33 \pm 5.2$ ms and $\tau = 91 \pm 15$ ms at +120 mV in control and CHT, respectively; n = 3). CHT modifications could not be reversed by washout with normal bath solution (not shown), but subsequent application of dithiothreitol (DTT) reversed them within 5-10 minutes (Fig. 1a. $\tau = 35 \pm 6.1$. n = 3). Unlike other A-type channels, KVS-1 possesses a domain in front of the inactivation domain, the N-Type Regulatory Domain (NIRD) which acts to slow N-type inactivation 11,12. Therefore, quantitative analysis was performed using a NIRD-deleted mutant (ΔNIRD) which inactivates faster than the wild type 11. CHT (Table S-1) or the more physiologically-relevant hydrogen peroxide (H_2O_2, Fig. 1b) slowed inactivation 10-fold, whereas DTT restored original kinetics. H_2O_2 and CHT led to a moderate (20 %) increase in the peak current and did not shift the half-maximal voltage for activation, $V_{1/2}$ (Table S-1).

KVS-1 cysteine 113 mediates redox effects

To determine which residues were modified by H_2O_2 and CHT we focused on the six endogenous cysteines of KVS-1 as the most likely candidates. Mutation of a conserved cysteine at position 113 in full-length KVS-1 or position 95 in ΔNIRD to serine (C113S,

ΔNIRD-C95S) yielded channels that were significantly resistant to H_2O_2 and CHT without affecting other channel attributes (C113S, Fig. 2a. $\tau = 30 \pm 4.2$ ms, $\tau = 38 \pm 5.4$ ms, and $\tau = 33 \pm 5.0$ at +120 mV in control, CHT and DTT, respectively; n = 3. ΔNIRD-C95S, Fig. 2b and Table S-1). Mutation of three other cysteines in the full-length channel (C151S and C209S located in the N-terminus; C283S in the middle of S2) did not affect the oxidant susceptibility of the channel; the C172S-C173S double-mutant expressed negligible currents and was not investigated further (data not shown). ΔNIRD-C95S channels exhibited a statistically significant residual response to oxidation (Table S-1) which may arise from oxidation of non-cysteine residues; this residual response was not investigated further here.

The accessory subunit MPS-1 does not affect redox modulation

In the nervous system of *C. elegans*, KVS-1 forms heteromeric complexes with the accessory subunit MPS-1 which acts to modulate functional attributes of the complex including inactivation 10. Complexes formed with MPS-1 and wild type KVS-1 (not shown) or ΔNIRD (Table S-1) retained susceptibility to CHT, and MPS-1 did not confer redox-susceptibility to C113S channels (not shown) or ΔNIRD-C95S channels (Table S-1). Taken together, these data indicated that mutation of a single cysteine, C113, made KVS-1 channels significantly resistant to oxidation and that the accessory subunit MPS-1 did not contribute to this modulation.

Normal and C113S genotypes respond differently to oxidative challenges

To probe the physiological role of the redox sensitivity of KVS-1 in the nervous system, we constructed transgenic worms expressing wild type or C113S KVS-1 under the *kvs-1* promoter (P_{kvs-1}) in a *kvs-1* knockout (*tm2034* strain) background. We named these transgenic worms, respectively, *wild type-KVS-1* and *C113S-KVS-1*, and assessed how oxidation challenges impacted their physiology. To this end we focused on chemotaxis to water-soluble attractants, a sensory function that is dependent on KVS-1 10. Chemotaxis is particularly amenable to study the effects that modifications in the function of KVS-1 have on behavior, because the electrical properties of the cells that mediate the primary chemotactic response (and which express KVS-1), the ASE neurons 13, have been extensivley charaterized *in vivo* 14. Furthermore several genetic tools including promoters that express exclusively in the ASE neurons 15,16, GFP reporters 15 and loss-of-function strains 17 are also available. Consistent with previous results obtained with RNA interference 10, *kvs-1* null worms exhibited defective chemotaxis to biotin (Fig. 3a) and lysine (data not shown). These phenotypes were suppressed in either *wild type-KVS-1* or *C113S-KVS-1* genotypes (Fig. 3a), confirming our transgenic approach.

Next, we investigated the effects of H_2O_2 or CHT on chemotaxis. Both oxidants (Fig. 3b-c), induced a significant loss of function in all genotypes (in average 70%) except in *C113S-KVS-1* in which loss was less marked (35%). These effects were not due to the attractant used because switching to lysine yielded similar results (70% versus 31%, only H_2O_2, n= 3 experiments, data not shown). Hydrogen peroxide also slightly affected chemotaxis to biotin in *kvs-1* KO worms (Fig. 3b). This indicates that there are cellular components independent of KVS-1, which contribute marginally to the oxidation-mediated decline in chemotaxis.

KVS-1 is expressed in ventral cord motor neurons which contribute to the worm's spontaneous locomotion 10. This raised the possibility that ROS-mediated impairment of locomotor function might have affected chemotaxis. To exclude and/or quantify possible effects due to defective locomotion we expressed wild type and C113S KVS-1 primarily in the ASE neurons by the means of the *flp-6* promoter, Pflp-6 16 (we named these transgenic worms $P_{flp\text{-}6}$*::wild type-KVS-1* and $P_{flp\text{-}6}$*::C113S-KVS-1*) and assessed their ability to perform chemotaxis to biotin, in normal conditions and after exposure to H_2O_2. The chemotactic response of the $P_{flp\text{-}6}$*::wild type-KVS-1* and $P_{flp\text{-}6}$*::C113S-KVS-1* worms recapitulated the response of the *wild type-KVS-1* and *C113S-KVS-1* genotypes (compare Fig. 3d with Fig. 3b) thereby excluding possible effects on chemotaxis due to defective motor neuron function and locomotion. To independently test the notion that chemotaxis was not affected by defects in locomotion we characterized the latter by counting thrashes 18 and by calculating the worm's average speed on solid substrate 19 (even though chemotaxis is also dependent upon the number of pirouettes and runs 20, these traits receive a significant contribution from the ASE neurons 21 and therefore alterations in these parameters would not necessarily reflect specific defects in spontaneous locomotion). Consistent with the observation that chemotaxis was normal in the $P_{flp\text{-}6}$*::wild type-KVS-1* and $P_{flp\text{-}6}$*::C113S-KVS-1* genotypes, both thrashing and average speed were also normal in *kvs-1* KO worms (Fig. 3 e-f). Moreover, thrashing and average speeds in the *wild type-KVS-1* and *C113S-KVS-1* genotypes recapitulated those in the *N2* genotype and most importantly, treatment with H_2O_2 did not cause a significant loss of locomotor function and affected all genotypes to the same extent (in average 10%). Together, these data suggest that the improved chemotactic response in *C113S-KVS-1* worms as well as the defective chemotaxis in *kvs-1* null worms is due to the specific contribution of this channel to ASE function rather than to an effect on motor neurons and locomotion. The fact that locomotion is normal in the *kvs-1* null genotype is probably a consequence of compensatory mechanisms that become activated when the expression of KVS-1 is suppressed.

The C113S mutant protects worms from chemosensory loss during ageing

Since ROS levels are thought to increase during ageing, we speculated that the chemotactic response should decline in old worms because of KVS-1 oxidation and, therefore, that C113S should attenuate this decline. Indeed, whereas ageing worms gradually lost the ability to perform chemotaxis to biotin (75% loss of function in 12 days), the C113S mutation significantly lessened this decline (40% loss, Fig. 4a). Similar results were observed for chemotaxis to lysine (70% versus 45%, n = 3, not shown). If oxidation of KVS-1 by ROS were responsible for the loss of chemosensory function associated with ageing, chemotaxis would be predicted to be preserved under conditions of low oxidative stress. We therefore employed the long-living *age-1(hx546)* mutant worm (TJ1052 strain) 22, which exhibits higher than normal levels of catalase and superoxide dismutase (SOD) activity 23-25 (Fig. 4f), as a positive control. Accordingly, in *age-1(hx546)* worms, loss of function was marginal and even less pronounced than in *C113S-KVS-1* worms, an effect probably due to the fact that in *age-1(hx546)* neurons many proteins besides KVS-1—including the receptors for biotin—are protected from the effects of ROS.

To further test the hypothesis that loss in chemosensory function in ageing worms was caused in part by oxidation of KVS-1, we treated them with DTT. Pre-incubation with DTT yielded a significant gain of function in *N2* or *wild type-KVS-1* worms (100%), whereas in *C113S-KVS-1* animals improvement was moderate (15%, Fig. 4b). Furthermore DTT did not significantly rescue the defective chemotactic response of *kvs-1* KO worms (C.I.= 0.17 ± 0.02 and 0.22 ± 0.03 in the absence/presence of DTT. n=2 experiments). To rule out the possibility that the chemotactic response of *C113S-KVS-1* worms might have been caused by preserved locomotion, we compared chemotaxis in four and twelve days old $P_{flp\text{-}6}$*::wild type-KVS-1* and $P_{flp\text{-}6}$*::C113S-KVS-1* worms (Fig. 4c) and counted thrashesand computed mean average speeds as done before (Fig. 4d-e). As expected, primary expression of C113S KVS-1 in the ASE neurons attenuated the age-related decline in chemosensory function (Fig. 4c). Furthermore, loss of locomotor function was similar in old *N2*, *wild type-KVS-1* and *C113S-KVS-1* worms, and moderate when compared to the decline in chemosensory function (25% versus 75%). This indicates that changes in spontaneous locomotion only marginally affected the decline in chemotaxis during ageing in these genotypes. The most likely explanation for the more modest loss of locomotor function in *age-1(hx546)* worms, is retarded muscle sarcopenia 26, an effect that might have contributed to the improved chemotactic response of this mutant.

To eliminate the possibility that differences in anti-oxidant defenses were causative in the enhanced chemotactic response in *C113S-KVS-1* worms, we measured the activity of SOD in four- and twelve-day-old worms. As expected, SOD activity was comparable in all genotypes and augmented in old worms (Fig. 4f). This latter observation is consistent with the notion that ROS levels were higher in old worms as it is thought that an increase in SOD activity reflects the response of the organism to oxidative stress in *C. elegans* as well as in mammals including *Homo sapiens* 27,28.

KVS-1 conducts the A-type current in the ASER neuron

To gain insight into the molecular mechanisms underlying the effects of ROS on chemosensory function we characterized the electrophysiology of native cells prepared from embryos, as morphological, electrophysiological, and GFP reporter studies have demonstrated that the differentiation and functional properties of cultured cells are similar to those observed *in vivo* 29-31. We recorded currents in the ASE right (ASER) neuron because this type of cell is the primary mediator of chemotaxis to water-soluble attractants 32. In Fig. 5a are shown exemplar currents expressed in *N2*, *wild type-KVS-1* and *C113S-KVS-1* ASER neurons four days after seeding and, for comparison, in an ASER neuron of *kvs-1* KO. The majority of *N2* cells (95%, n= 38) exhibited robust, voltage-dependent A-type currents which recapitulated native currents expressed in dissected ASER neurons 14. Substitution of *N*-methyl-d-glucamine for K^+ in the pipette solution abolished outward currents (data not shown) suggesting that they were carried by K^+ ions. Inactivation was voltage-dependent and rapid in *N2* neurons (Fig. 5b). In contrast, currents expressed in neurons from *tm2034* worms (n=23) did not inactivate (aside from two cells expressing a small inactivating current), were ∼ 50% smaller (Fig. 5c), and activated at more positive voltages (Table S-2). Consistent with the fact that *wild type-KVS-1* and *C113S-KVS-1* worms exhibited normal chemotaxis, the currents expressed in neurons from these animals

fully recapitulated the currents in *N2* neurons (Fig. 5, Table S-2) suggesting that little if any overexpression of KVS-1 occurred in the transgenic worms. Taken together, these data indicated that KVS-1 conducts the A-type current in ASER neurons in agreement with previous data obtained with *kvs-1* RNAi 33. However, heterologously expressed KVS-1 channels, alone or with the accessory subunit MPS-1, do not completely recapitulate native channels. There is a -40 mV shift in the $V_{1/2}$ of native currents compared to heterologously expressed currents and the kinetics of inactivation are ∼ 2-fold faster in native than in mammalian cells. We do not have a definitive explanation for these discrepancies, but they may reflect differences in plasma membrane composition, the presence of unidentified subunits in native complexes, or lack of the NIRD. We contend these differences are post-translational in origin, because *wild type-KVS-1* and *C113S-KVS-1* worms express currents with native attributes. We found another discrepancy between the attributes of heterologous and native KVS-1 channels. Recently, it has been shown that KVS-1 exhibits cumulative activation (CA) when expressed in *Xenopus laevis* oocytes but not in mammalian cells 34. We tested whether native currents exhibited CA, but failed to observe this phenomenon *in vivo* (not shown). This suggests that CA is an effect dependent on the *Xenopus laevis* expression system.

Oxidizing agents modify native KVS-1 channels

The fact that KVS-1 conducts the A-type current in ASER suggests that native currents are susceptible to oxidation. As expected, application of H_2O_2 in the bath solution quickly converted inactivating currents—expressed in 4-day-old neurons—into non-inactivating currents (Fig 6a). As a consequence of the slowed inactivation of KVS-1, the magnitude of the steady-state current dramatically increased. Thus, the fractional current, obtained by dividing the current at the end of the test pulse by the peak current (if the current inactivated) or by the current 5 ms after the beginning of the test pulse (if the current did not inactivate), I_{steady} /$I_{beginning}$, increased from 0.55 ± 0.02 (control) to 1.04 ± 0.07 (after exposure to H_2O_2, n = 3 cells, Fig. 6a). For quantitative analysis, we recorded currents in the presence of oxidizing agents in the pipette solution. Thus, in *N2* and *wild type-KVS-1*, adding H_2O_2 or CHT to the pipette solution suppressed inactivation and resulted in a 2-fold increase in the fractional current (Fig. 6b). Neither H_2O_2 nor CHT significantly altered the currents expressed in *C11 3S-KVS-1* ASER neurons (Fig. 6b). Furthermore, H_2O_2 did not modify the *tm2034* current (Fig. S-1, supplementary information), indicating that the KVS-1 current is the only component of the ASER K^+ current susceptible to redox modulation.

Endogenous ROS modify native KVS-1 channels

The fact that native currents can be modified by oxidizing agents argues that endogenous ROS may cause significant electrical remodeling in native cells by acting to oxidize KVS-1 channels during ageing. In this case, old neurons should exhibit non-inactivating K^+ currents, similar to those expressed in young neurons exposed to oxidizing agents. In fact, the percentage of *N2* ASER neurons expressing fast-inactivating currents (fractional current < 0.75), which was 95 % at day 4, decreased to 41 % ($P < 0.0001$) at day 12. The majority of these old neurons (59 %) expressed non-inactivating currents, as those shown in Fig. 7a. The functional properties of these non-inactivating currents are listed in Table S-2. The slowing of inactivation led to a significant increase in the magnitude of the steady-state

current (inset of Fig. 7a)—an effect with potentially significant physiological consequences (see below) and which was reflected in the doubling of the mean fractional current (Fig. 7b)—without affecting other gating properties such as the voltage-dependence of activation (Table S-2). Furthermore, non-inactivating currents were also expressed in 12-day-old *wild type-KVS-1* ASER neurons in percentages similar to those of *N2* cells (54 %, compared to 8 % at day 4, $P < 0.0001$. Fig. 7a-b, Table S-2). In contrast, both *C113S-KVS-1* and *age-1(hx546)* neurons seldom expressed non-inactivating currents (from 4 % at day 4 to 17 % at day 12 in *C113S-KVS-1*; from 7 % to 20 % in *age-1(hx546)*), nor did their mean fractional currents change appreciably during ageing (Fig. 7a-b). Neither were currents in 12-day-old *tm2034* neurons significantly modified (Fig. S-1 supplementary information and Table S-2). To corroborate the notion that in old neurons the modifications in the KVS-1 current were caused by oxidation of KVS-1—presumably by endogenous ROS—we recorded in the absence/presence of DTT. Thus, in 12-day-old *N2* neurons, application of 0.3 mM DTT in the bath solution (Fig. 7c) restored inactivation. Moreover, when DTT was present in the pipette solution the number of fast inactivating currents (fractional current < 0.75) rose dramatically (Fig. 7d) in both *N2* (from 43 % to 100 % $P < 0.0001$) and *wild type-KVS-1* (from 42 % to 92 % $P < 0.0001$).

To determine how oxidation of KVS-1 impacted ASER neuron electrical signaling we recorded potentials evoked in these cells by current injections. To correlate the oxidation status of KVS-1 with the voltage response of the neuron, we recorded the potentials and the whole-cell currents in the same cell. Exemplar potentials elicited in a four days old *N2* ASER neuron in response to current injections from -4 pA to +20 pA in 4 pA increments (Fig. 7g inset) are shown in Fig. 7e. The corresponding whole-cell currents, recorded immediately after the potentials, are shown in the inset of the figure. Depolarization was graded with stimulus amplitude and saturated at +78 mV from a resting potential of -55 mV (Fig. 7g). These voltage responses were markedly non-linear. The cell depolarized quickly up to roughly 0 mV. Above this threshold the neuron depolarized considerably more slowly, giving rise to a characteristic bi-phasic response. These voltage responses recapitulated the potentials recorded in native ASER neurons 14 thereby further validating the use of cultured neurons for electrophysiological studies. As expected, the voltage responses in 12 days old neurons (Fig. 7f), expressing non-inactivating currents (inset), or in four days old neurons recorded in the presence of 0.25 mM H_2O_2 in the patch pipette (Table 1), were markedly different. First, the maximum depolarization attained by old cells at steady-state was significantly decreased (38 mV, Fig. 7g. See also Table 1). Second, the cell depolarized significantly faster (4-fold) without the characteristic bi-phasic kinetics (Fig. 7f and Table 1). Rise times in four and twelve days old *kvs-1* null neurons were also significantly faster and mono-phasic compared to *N2* neurons (Table 1, Fig. S-1), indicating that under normal conditions, the A-type current conducted by KVS-1 is responsible for the kinetics of activation of the ASER voltage response. Because the current in ASER neurons expressing C113S KVS-1 does not appreciably change during ageing or in the presence of oxidizing agents, also the voltage responses in this genotype should not change. As expected, the potentials elicited in *C113S KVS-1* ASERs recapitulated those in *N2* neurons at day four and did not significantly change during ageing (Fig. 7g) nor in the presence of H_2O_2 (Table 1).

Together these data establish a direct link between oxidative regulation of KVS-1 function during ageing and ASER neuron signaling.

In summary, both the resistance of KVS-1 to oxidation (conferred by the C113S mutation) and the increased anti-oxidant defenses in *age-1(hx546)*, acted to prevent modification of the ASER K^+ current by ROS during ageing and as a consequence, ASER excitability. These findings indicate that primary ASER neurons are subject to normal ageing processes, even though the levels of ROS in cultured neurons and *in vivo* may be different. We conclude that oxidation of KVS-1 by ROS represents a significant cause of electrical remodeling in the ASE neurons, a fact that provides a natural explanation for the progressive loss in chemosensory function in the animal during ageing.

DISCUSSION

To answer fundamental questions about the role played by physiological interactions of ROS with K^+ channels in regulating neuronal function, we developed a *C. elegans* animal model system of K^+ channel-mediated protection from oxidative stress using voltage-gated K^+ channel KVS-1 and a redox-resistant variant, C113S. We find that altered neuronal excitability, via ROS-mediated modification of KVS-1, is a significant cause of sensorial decline during ageing in *C. elegans*. Thus, chemotaxis to biotin and lysine—a sensory function controlled by KVS-1—progressively declined in ageing worms. This loss was mimicked by exposing young worms to oxidizing agents and reversed by treating old worms with DTT. By contrast, loss of chemosensory function was significantly lessened in worms harboring the C113S variant (even though their SOD levels were not different) and in *age-1(hx546)* worms, which overexpress anti-oxidant defenses. Since we measured the activity of SOD in the entire animal, we cannot rule out the possibility that SOD levels changed only in the neurons expressing KVS-1, although this seems very unlikely.

Electrophysiological analyses showed that the native potassium current in the ASER neuron, a cell that mediates chemotaxis to biotin and lysine, was altered by both endogenous and exogenous ROS via specific modification of KVS-1 channels whereas in neurons expressing C113S, or in conditions of low oxidative stress in the *age-1(hx546)* genotype, the current was modified very little. As expected, oxidative modifications in the KVS-1 current had a profound impact on ASER excitability by acting to alter both the transient and steady-state characteristics of its voltage responses.

The effects of oxidation of KVS-1 were most easily noticed at voltages that generally are outside the physiological range of vertebrate cells. However, it appears to be a common property of *C. elegans* neurons and muscles to work at more positive voltages than the cells of other species; consequently, potassium channels activate at more depolarizing voltages than their mammalian homologs 14,35-40. Our data showed that the ASER neuron is extremely responsive to input currents because currents of few pA could depolarize this cell by tens of mV. Thus, the opening of a few receptor channels in the physiological range, can significantly depolarize this cell. In conclusion these data show that KVS-1 conducts a current that has a profound impact on the signaling ability of the ASER. A detailed

investigation of the mechanisms by which KVS-1 shapes ASER neuron signaling are beyond the scope of this study and will be the matter of a future study.

While our data underscore a prominent role of C113 in the molecular mechanism by which redox-modifications slow KVS-1 inactivation, it remains to be determined whether oxidation of this residue leads to formation of disulfide cysteines (between two C113 or alternatively with a cysteine in the C172-C173 pair) or alternatively sulfinic or sulfonic acid. Residues other than cysteines, methionines for example, are not likely to play a role because they would not be reduced by DTT 41. Further investigations will address this issue.

Evidence has been accumulating in the past years that ageing in mammalian neurons is associated with changes in K^+ homeostasis 42,43. In particular, cortical neurons deficient in Kv2.1 channels (a KVS-1 homolog), are protected from oxidant-induced apoptosis *in vitro* 44. The fact that elevated levels of ROS are found in the aging brain 45, and that ROS-induced neurodegeneration is a condition of many neuronal pathologies including Alzheimer's disease 46 and multiple sclerosis, 47 prompts the intriguing concept that the chain of events leading to age-related neurodegeneration in the nervous system of mammals could involve the interaction of ROS with K^+ channels. Thus, oxidative modification of K^+ channels might represent a fundamental pathogenic mechanism in mammals.

In summary, we report an exquisitely simple physiological process through which voltage-gated K^+ channels lead to sensorial decline during ageing. Considering that K^+ channels and ROS are universal players in the biological game we put forward the intriguing idea that physiological oxidation of voltage-gated K^+ channels may represent a common pathogenic mechanism in biological organisms.

METHODS SUMMARY

Strain used were: Bristol (*N2*), tm2034, age-1(hx546), eat-4(ky5), tm2034(P_{KVS-1}::KVS-1)(myo-2::gfp), termed wild type-KVS-1, tm2034(P_{KVS-1}::C113S-KVS-1)(myo-2::gfp), termed C113S-KVS-1, tm2034(P_{KVS-1}::KVS-1)(myo-2::gfp)(gcy-5::gfp)(rol-6), tm2034(P_{KVS-1}::C113S-KVS-1)(myo-2::gfp)(gcy-5::gfp)(rol-6), age-1(hx546)(gcy-5::gfp)(rol-6), tm2034(Pf_{lp-6}::KVS-1)(myo-2::gfp)(gcy-5::gfp) and *tm2034(Pf_{lp-6}::C113S)(myo-2::gfp)(gcy-5::gfp)*.

A 3162 bp fragment (termed the promoter of *kvs-1* or P_{kvs-1}) was amplified by PCR from the C53C9 cosmid and subcloned in the the pPD95.75 Fire vector (*P_{kvs-1}::gfp* construct) alone or with the cDNA of KVS-1 (*wild type-KVS-1*) or C113S (*C113S-KVS-1*). Transformant lines for *wild type-KVS-1* and *C113S-KVS-1* were integrated by γ-ray (4000 rads for 40 minutes). *P_{kvs-1}::gfp* yielded GFP signals in several amphid neurons including the ASEs, vulva, ventral cord motor-neurons and anal depressor muscle 10 (Fig. S-2). 2481 bp of genomic DNA (termed the promoter of *flp-6*, or P_{flp-6}) were amplified by PCR and subcloned in a construct containing the cDNA of KVS-1 (*P_{flp-6}::wild type-KVS-1*) or C113S (*P_{flp-6}::C113S-KVS-1*) in the the pPD95.75 vector.

Behavioral tests were performed without knowledge of the worms' genotype and were performed as described previously 10. Ageing experiments were started with ~600-1000

age-synchronized worms per genotype (except with *Pflp-6::wild type-KVS-1* and *Pflp-6::C113S-KVS-1*, which were started with ∼200-300 age-synchronized worms). Worms were examined every day until death and were scored as dead when they were no longer able to move even in response to prodding with a platinum pick.

Quantitative data are presented as mean ± standard error of the mean (s.e.m).

Supplementary Material

Refer to Web version on PubMed Central for supplementary material.

Acknowledgements

We thank Dr. Shohei Mitani for the *tm2034* strain, Dr. Oliver Hobert for the *Pgcy-5::GFP* construct and the *C. elegans* Knock-Out Consortium for the TJ1052 strain. We thank Drs. Andrew Jauregui and Maureen Barr for their help with the average speed measurements.and Drs. John Lenard, Geoffrey Abbott and Loren Runnels for critical reading of the manuscript. This work was supported by a NIH grant (R01GM68581) to FS.

REFERENCES

1. Harman D. Aging: a theory based on free radical and radiation chemistry. J Gerontol. 1956; 11:298–300. [PubMed: 13332224]
2. Annunziato L, et al. Modulation of ion channels by reactive oxygen and nitrogen species: a pathophysiological role in brain aging? Neurobiol Aging. 2002; 23:819–34. [PubMed: 12392785]
3. Ruppersberg JP, et al. Regulation of fast inactivation of cloned mammalian IK(A) channels by cysteine oxidation. Nature. 1991; 352:711–4. [PubMed: 1908562]
4. Duprat F, Girard C, Jarretou G, Lazdunski M. Pancreatic two P domain K+ channels TALK-1 and TALK-2 are activated by nitric oxide and reactive oxygen species. J Physiol. 2005; 562:235–44. [PubMed: 15513946]
5. Tang XD, Garcia ML, Heinemann SH, Hoshi T. Reactive oxygen species impair Slo1 BK channel function by altering cysteine-mediated calcium sensing. Nat Struct Mol Biol. 2004; 11:171–8. [PubMed: 14745441]
6. Zeidner G, Sadja R, Reuveny E. Redox-dependent gating of G protein-coupled inwardly rectifying K+ channels. J Biol Chem. 2001; 276:35564–70. [PubMed: 11466316]
7. Avshalumov MV, Rice ME. Activation of ATP-sensitive K+ (K(ATP)) channels by H2O2 underlies glutamate-dependent inhibition of striatal dopamine release. Proc Natl Acad Sci U S A. 2003; 100:11729–34. [PubMed: 13679582]
8. Gamper N, et al. Oxidative modification of M-type K(+) channels as a mechanism of cytoprotective neuronal silencing. Embo J. 2006; 25:4996–5004. [PubMed: 17024175]
9. Kenyon, C., editor. Environmental factors and gene activities that influence life span. Cold Spring Harbor Laboratory Press; Cold Spring Harbor: 1997.
10. Bianchi L, Kwok SM, Driscoll M, Sesti F. A potassium channel-MiRP complex controls neurosensory function in Caenorhabditis elegans. J Biol Chem. 2003; 278:12415–24. [PubMed: 12533541]
11. Cai SQ, Sesti F. A new mode of regulation of N-type inactivation in a Caenorhabditis elegans voltage-gated potassium channel. J Biol Chem. 2007; 282:18597–601. [PubMed: 17488718]
12. Hoshi T, Zagotta WN, Aldrich RW. Biophysical and molecular mechanisms of Shaker potassium channel inactivation. Science. 1990; 250:533–8. [PubMed: 2122519]
13. Bargmann, C.; Mori, I. C. elegans II. Riddle, DL.; B, T.; Meyer, BJ.; Priess, JR., editors. Cold Spring Harbor Laboratory Press; Cold Spring Harbor: 1997. p. 717-37.
14. Goodman M, Hall D, Avery L, Lockery S. Active currents regulate sensitivity and dynamic range in C. elegans neurons. Neuron. 1998; 20:763–72. [PubMed: 9581767]

15. Yu S, Avery L, Baude E, Garbers D. Guanylyl cyclase expression in specific sensory neurons: a new family of chemosensory receptors. Proc. Natl. Acad. Sci USA. 1997; 94:3384–7. [PubMed: 9096403]
16. Kim K, Li C. Expression and regulation of an FMRFamide related neuropeptide gene family in Caenorhabditis elegans. J. Comp. Neurol. 2004; 475:540–50. [PubMed: 15236235]
17. Lee RY, Sawin ER, Chalfie M, Horvitz HR, Avery L. EAT-4, a homolog of a mammalian sodium-dependent inorganic phosphate cotransporter, is necessary for glutamatergic neurotransmission in caenorhabditis elegans. J Neurosci. 1999; 19:159–67. [PubMed: 9870947]
18. Miller K, et al. A genetic selection for Caenorhabditis elegans synaptic transmission mutants. Proc Natl Acad Sci U S A. 1996; 93:12593–8. [PubMed: 8901627]
19. Ramot D, Johnson BE, Berry TL Jr. Carnell L, Goodman MB. The Parallel Worm Tracker: a platform for measuring average speed and drug-induced paralysis in nematodes. PLoS ONE. 2008; 3:e2208. [PubMed: 18493300]
20. Pierce-Shimomura JT, Morse TM, Lockery SR. The fundamental role of pirouettes in Caenorhabditis elegans chemotaxis. J Neurosci. 1999; 19:9557–69. [PubMed: 10531458]
21. Suzuki H, et al. Functional asymmetry in Caenorhabditis elegans taste neurons and its computational role in chemotaxis. Nature. 2008; 454:114–8. [PubMed: 18596810]
22. Klass MR. A method for the isolation of longevity mutants in the nematode Caenorhabditis elegans and initial results. Mech Ageing Dev. 1983; 22:279–86. [PubMed: 6632998]
23. Lithgow GJ, White TM, Melov S, Johnson TE. Thermotolerance and extended life-span conferred by single-gene mutations and induced by thermal stress. Proc Natl Acad Sci U S A. 1995; 92:7540–4. [PubMed: 7638227]
24. Vanfleteren JR. Oxidative stress and ageing in Caenorhabditis elegans. Biochem J. 1993; 292(Pt 2):605–8. [PubMed: 8389142]
25. Larsen PL. Aging and resistance to oxidative damage in Caenorhabditis elegans. PNAS. 1993; 90:8905–09. [PubMed: 8415630]
26. Herndon LA, et al. Stochastic and genetic factors influence tissue-specific decline in ageing C. elegans. Nature. 2002; 419:808–14. [PubMed: 12397350]
27. Darr D, Fridovich I. Adaptation to oxidative stress in young, but not in mature or old, Caenorhabditis elegans. Free Radic Biol Med. 1995; 18:195–201. [PubMed: 7744302]
28. Okabe T, Hamaguchi K, Inafuku T, Hara M. Aging and superoxide dismutase activity in cerebrospinal fluid. J Neurol Sci. 1996; 141:100–4. [PubMed: 8880700]
29. Christensen M, et al. A primary culture system for functional analysis of C. elegans neurons and muscle cells. Neuron. 2002; 33:503–14. [PubMed: 11856526]
30. Zhang Y, et al. Identification of genes expressed in C. elegans touch receptor neurons. Nature. 2002; 418:331–5. [PubMed: 12124626]
31. Suzuki H, et al. In vivo imaging of C. elegans mechanosensory neurons demonstrates a specific role for the MEC-4 channel in the process of gentle touch sensation. Neuron. 2003; 39:1005–17. [PubMed: 12971899]
32. Bargmann CI, Horvitz HR. Chemosensory neurons with overlapping functions direct chemotaxis to multiple chemicals in C. elegans. Neuron. 1991; 7:729–42. [PubMed: 1660283]
33. Park KH, Hernandez L, Cai SQ, Wang Y, Sesti F. A Family of K+ Channel Ancillary Subunits Regulate Taste Sensitivity in Caenorhabditis elegans. J Biol Chem. 2005; 280:21893–9. [PubMed: 15799965]
34. Rojas P, et al. Cumulative activation of voltage-dependent KVS-1 potassium channels. J Neurosci. 2008; 28:757–65. [PubMed: 18199775]
35. Santi CM, et al. Dissection of K+ currents in Caenorhabditis elegans muscle cells by genetics and RNA interference. Proc Natl Acad Sci U S A. 2003; 100:14391–6. [PubMed: 14612577]
36. Ramot D, MacInnis BL, Goodman MB. Bidirectional temperature-sensing by a single thermosensory neuron in C. elegans. Nat Neurosci. 2008; 11:908–15. [PubMed: 18660808]
37. Richmond JE. Electrophysiological recordings from the neuromuscular junction of C. elegans. WormBook. 2006:1–8. [PubMed: 18050434]

38. Jospin M, Mariol M, Segalat L, Allard B. Characterization of K+ currents using an in situ patch-clamp technique in body wall muscle cells from Caenorhabditis elegans. J of Physiol. 2002
39. Richmond JE, Jorgensen EM. One GABA and two acetylcholine receptors function at the C. elegans neuromuscular junction. Nat Neurosci. 1999; 2:791–7. [PubMed: 10461217]
40. Mellem JE, Brockie PJ, Madsen DM, Maricq AV. Action potentials contribute to neuronal signaling in C. elegans. Nat Neurosci. 2008; 11:865–7. [PubMed: 18587393]
41. Ciorba MA, Heinemann SH, Weissbach H, Brot N, Hoshi T. Modulation of potassium channel function by methionine oxidation and reduction. Proc Natl Acad Sci U S A. 1997; 94:9932–7. [PubMed: 9275229]
42. Alshuaib WB, et al. Reduced potassium currents in old rat CA1 hippocampal neurons. J Neurosci Res. 2001; 63:176–84. [PubMed: 11169627]
43. Yu SP, et al. Mediation of neuronal apoptosis by enhancement of outward potassium current. Science. 1997; 278:114–7. [PubMed: 9311914]
44. Pal S, Hartnett KA, Nerbonne JM, Levitan ES, Aizenman E. Mediation of neuronal apoptosis by Kv2.1-encoded potassium channels. J Neurosci. 2003; 23:4798–802. [PubMed: 12832499]
45. Serrano F, Klann E. Reactive oxygen species and synaptic plasticity in the aging hippocampus. Ageing Res Rev. 2004; 3:431–443. [PubMed: 15541710]
46. Behl C. Alzheimer's disease and oxidative stress: implications for novel therapeutic approaches. Prog Neurobiol. 1999; 57:301–323. [PubMed: 10096843]
47. Bo L, et al. Induction of nitric oxide synthase in demyelinating regions of multiple sclerosis brains. Ann Neurol. 1994; 36:778–86. [PubMed: 7526776]

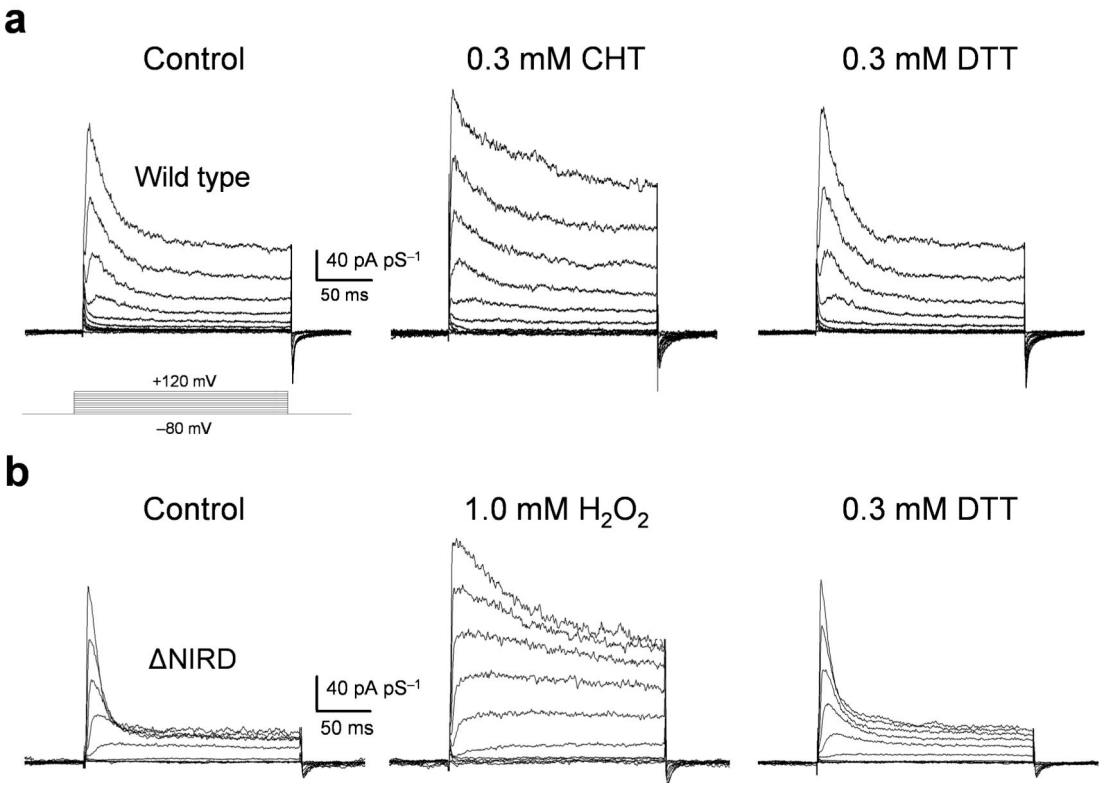

Fig. 1. KVS-1 channels expressed in mammalian cells are susceptible to redox modulation

A Representative macroscopic KVS-1 currents elicited by voltage jumps from -80 mV to +120 mV in 20 mV increments (inset) in control and after application of 0.3 mM CHT for five minutes in the test solution, washout and application of 0.3 mM DTT for 5-10 minutes in the test solution.

B Representative ΔNIRD currents in control and after application of 1 mM H_2O_2 for 2-3 minutes, washout, and application of 0.3 mM DTT for 5-10 minutes.

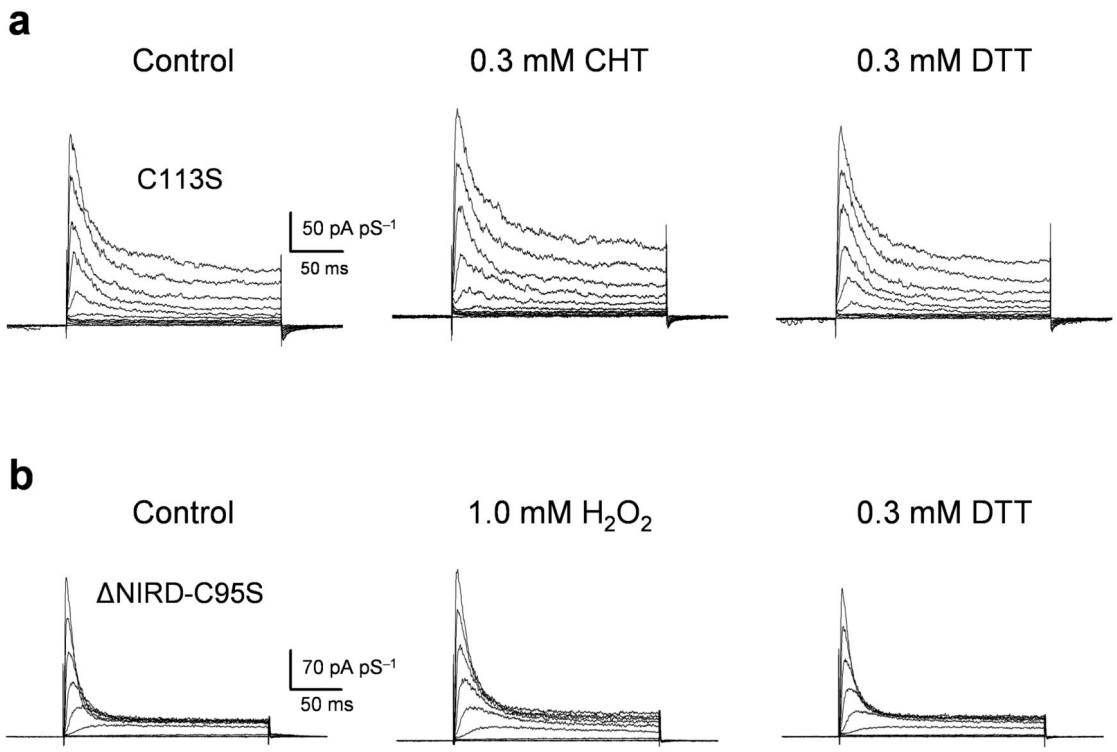

Fig. 2. Cysteine 113 mediates redox modulation of KVS-1

A Representative macroscopic C113S KVS-1 currents elicited by voltage jumps from -80 mV to +120 mV in 20 mV increments in control and after application of 0.3 mM CHT for 5 minutes in the test solution, washout and application of 0.3 mM DTT for 5-10 minutes in the test solution.

B Representative ΔNIRD-C95S currents in control and after application of 1 mM H_2O_2 for 2-3 minutes, washout, and application of 0.3 mM DTT for 5-10 minutes.

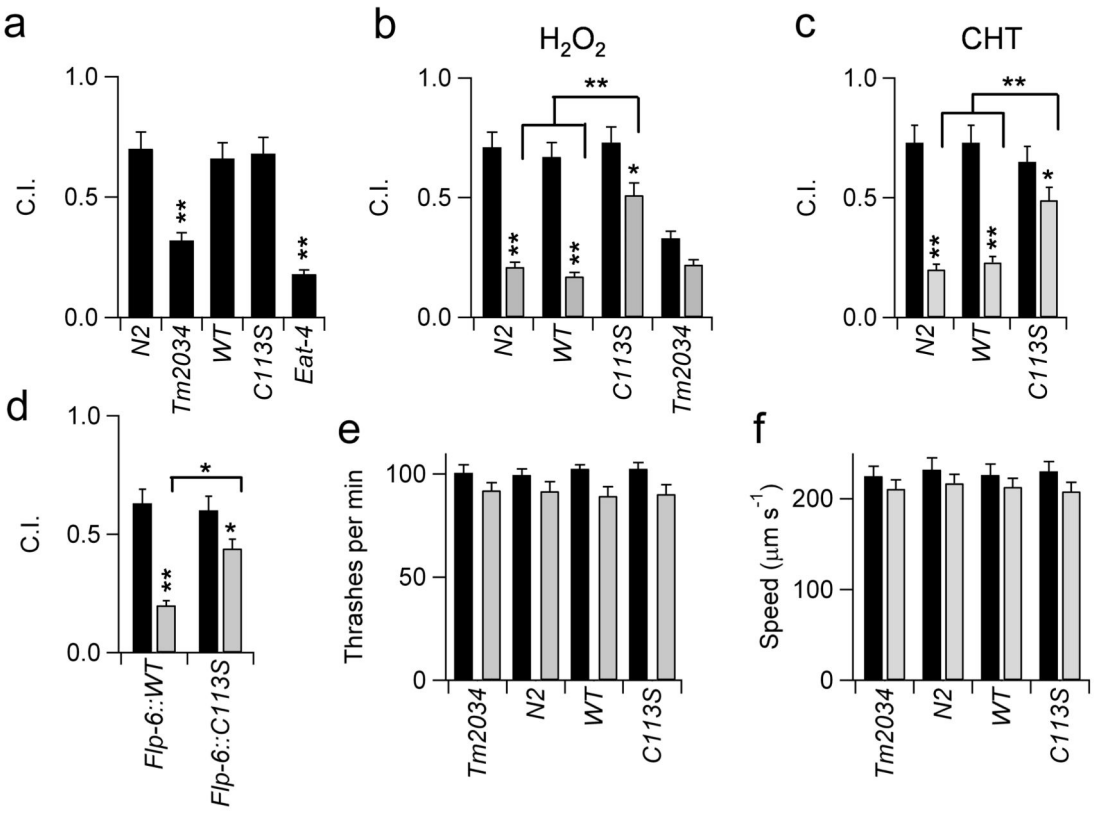

Fig. 3. Protected chemosensory function in C113S worms

A Chemotaxis to biotin in *N2* (parental control strain), *tm2034* (*kvs-1* null), *wild type-KVS-1* (WT) and *C113S-KVS-1* (C113S), L4 worms. The chemotaxis-defective *eat-4(ky5)*, which harbors a mutation in a vesicular glutamate transporter necessary for glutamatergic neurotransmission in *C.elegans*, was employed as "sensory-defective" positive control 17. n = 4 experiments.

B Chemotaxis to biotin in control conditions (black) and in worms exposed to hydrogen peroxide (light grey). Young adult worms were soaked in M9 buffer containing 1 mM H_2O_2 (for 20 minutes) or M9 buffer (control), allowed to recover for 30 minutes 25, transferred to a test plate and tested for chemotaxis. n = 5 experiments for *N2*, *wild type-KVS-1* and *C113S-KVS-1* and n = 3 experiments for *kvs-1* KO.

C As in B for worms exposed to 0.5 mM CHT for 40 minutes. n = 5 experiments.

D As in B for $P_{flp\text{-}6}$*::wild type-KVS-1* and $P_{flp\text{-}6}$*::C113S-KVS-1* worms. n = 4 experiments.

E Forward movement phenotype in the indicated genotypes in control (black) and after exposure to 1 mM H_2O_2 (light grey). n ≥ 11 animals/bar.

F Mean average speeds in the indicated genotypes in control (black) and after exposure to 1 mM H_2O_2 (light grey). n ≥ 10 animals/bar.

Data are presented as mean ± standard error of the mean (s.e.m). Statistically significant differences are indicated with * ($0.01 < P < 0.05$) and ** ($P < 0.01$).

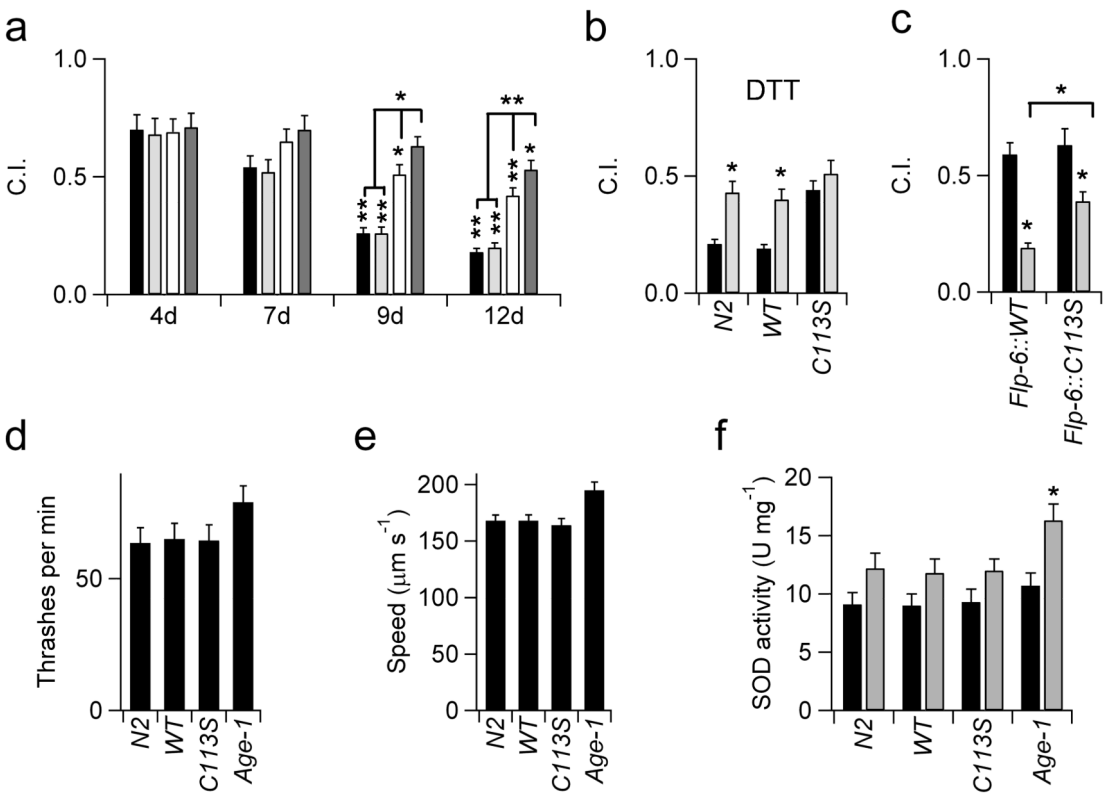

Fig. 4. Chemosensory loss is lessened in C113S worms during ageing

A Chemotaxis to biotin in the indicated genotypes (*N2* black, *wild type-KVS-1* light grey, *C113S-KVS-1* white, *age-1(hx546)* dark grey) at the indicated time points. T= 20 °C. An experiment started with 600-1000 age-synchronized worms/genotype that were scored for chemotaxis at the indicated time points (∼100 worms/time point). *N2*, *wild type-KVS-1* and *C113S-KVS-1*, n = 8 experiments. *Age-1(hx546)*, n = 3 experiments.

B Chemotaxis to biotin in control conditions (black) and in worms exposed to DTT (light grey). Twelve days old worms were soaked in M9 buffer + 1 mM DTT orM9 buffer (control) for 30 minutes, allowed to recover for 1-2 hours, transferred to a test plate and tested for chemotaxis. n=3 experiments.

C Chemotaxis to biotin in four days (black) and 12 days (light grey) old $P_{flp\text{-}6}$*::wild type-KVS-1* and $P_{flp\text{-}6}$*::C113S-KVS-1* worms. n = 3 experiments.

D Forward movement phenotype in the indicated genotypes in 12 days old worms. n ≥ 11 animals/bar.

E Mean average speed in the indicated genotypes in 12 days old worms. n ≥ 10 animals/bar.

F SOD activity in 4 (black) and 12 days old (light grey) worms. SOD activity was normalized to the total protein content of the lysate. n = 3 experiments.

Data are presented as mean ± standard error of the mean (s.e.m). Statistically significant differences are indicated with * ($0.01 < P < 0.05$) and ** ($P < 0.01$).

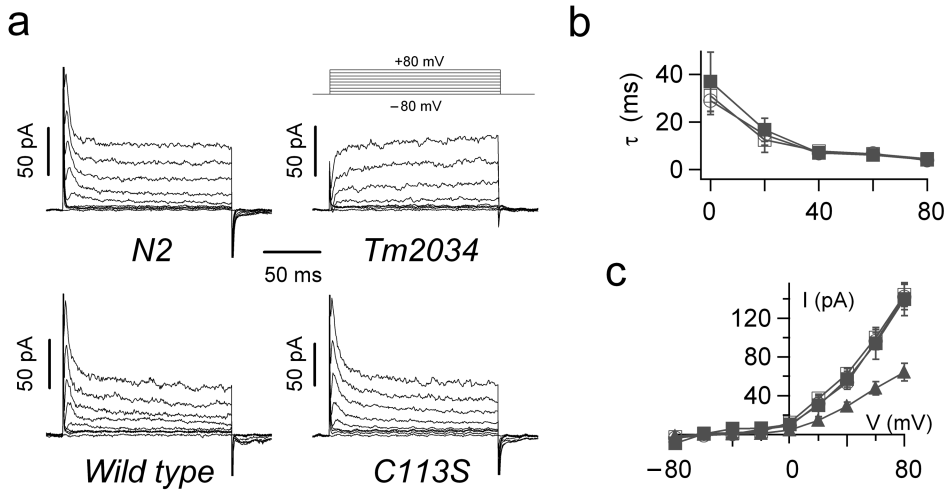

Fig. 5. KVS-1 conducts the A-type current in ASER neurons

A Representative whole-cell currents elicited by voltage jumps from -80 mV to +80 mV (inset) in *N2*, *wild type-KVS-1*, *C113S-KVS-1* and *tm2034* ASER neurons. Currents were recorded four days after seeding.

B Inactivation rates in *N2* (hollow squares), *wild type-KVS-1* (squares) and *C113S-KVS-1* (hollow circles) currents. Time constants were calculated by fitting macroscopic currents to a single exponential function (eqn. S-1). n= 38, 13 and 25 cells for respectively *N2*, *wild type-KVS-1* and *C113S-KVS-1*.

C Peak current-voltage relationships in ASER neurons of *N2*, *wild type-KVS-1*, *C113S-KVS-1* worms and steady-state current-voltage relationship in ASER neurons of *tm2034* worms (triangles). n = 38, 13, 25 and 23 cells for respectively *N2*, *wild type-KVS-1*, *C113S-KVS-1* and *tm2034*.

ASER neurons were marked by the *Pgcy-5::gfp* reported which specifically expresses in this neuron type 15.

Data are presented as mean ± standard error of the mean (s.e.m).

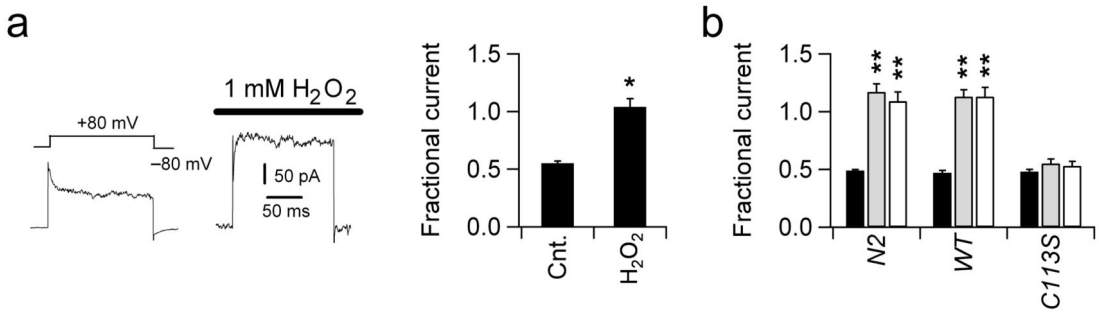

Fig. 6. Native KVS-1 currents are modified by oxidizing agents

A Representative whole-cell currents evoked in a four days old *N2* ASER neuron by single voltage jumps from -80 mV to +80 mV (inset) before and after application of 1 mM H_2O_2 in the bath solution. Right, fractional current, $I_{steady}/I_{beginning}$, at +80 mV before and after exposure to 1 mM H_2O_2, n = 3 cells.

B Fractional currents at +80 mV in four days old *N2*, *wild type-KVS-1* and *C113S-KVS-1* neurons in the absence (black, n = 15, 14 and 11 cells, respectively) and presence of 0.25 mM H_2O_2 (light grey, n = 12, 11 and 9 cells respectively) or 0.25 mM CHT (white, n = 10, 11 and 5 cells respectively) in the patch pipette.

Data are presented as mean ± standard error of the mean (s.e.m). Statistically significant differences are indicated with * ($0.01 < P < 0.05$) and ** ($P < 0.01$).

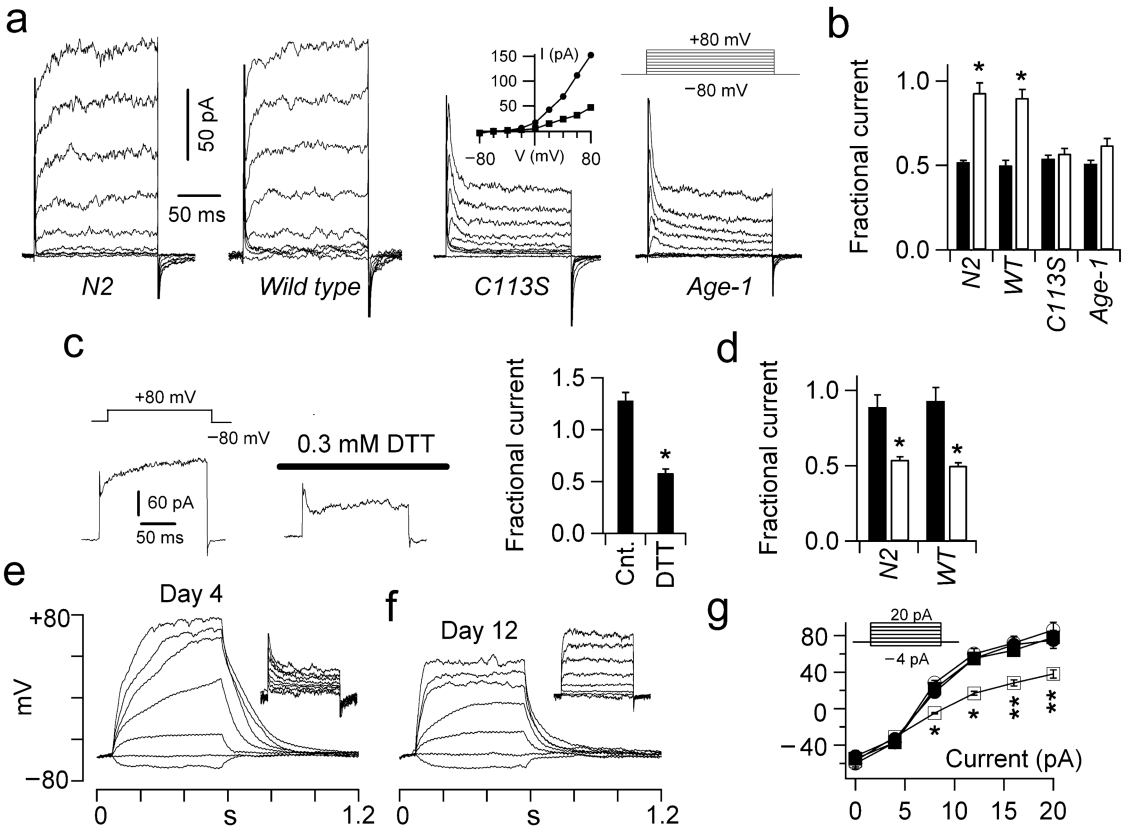

Fig. 7. Native KVS-1 currents are modified by endogenous ROS

A Representative whole-cell currents elicited by single voltage jumps from -80 mV to +80 mV (inset) in a 12 days old *N2*, *wild type-KVS-1*, *C113S-KVS-1* and *age-1(hx546)* ASER neuron. Inset, representative steady-state current-voltage relationships in 12 days *N2* (squares) and *C113S-KVS-1* (circles) cells.

B Mean fractional current at +80 mV, in 4 days (black) and 12 days (light grey) old neurons in the *N2*, *wild type-KVS-1*, *C113S-KVS-1* and *age-1(hx546)* genotypes. Number of cells, are, n = 38, 13, 25 and 15 respectively at day 4 and n = 29, 24, 23 and 15 cells respectively at day 12.

C Representative whole-cell currents evoked in an *N2* ASER neuron by single voltage jumps from -80 mV to +80 mV (inset) before and after application of 0.3 mM DTT in the bath solution. Right, fractional current at +80 mV before and after exposure to DTT, n = 3 cells.

D Mean fractional current in 12 days old *N2* or *wild type-KVS-1* neurons recorded in the absence (black, n = 21 and 19 cells, respectively) or presence of 0.2 mM DTT in the pipette solution (light grey, n = 12 and 13 cells, respectively).

E Representative potentials evoked in a 4 days old *N2* ASER cultured neuron in response to 0.5 s current injections from -4 pA to 20 pA in 4 pA increments (current protocol in the inset of **Fig. 7 f**). Inset, whole-cell currents recorded in the same cell evoked by 1 s voltage steps from -80 mV to +80 mV in 20 mV increments.

F As in (E) in a 12 days old *N2* ASER neuron.

G Steady-state voltage-current relationships in 4 days old *N2* neurons (filled squares, fractional current = 0.49 ± 0.08, n = 8 cells), 12 days old *N2* neurons (hollow squares,

fractional current 0.98 ± 0.07, n = 7 cells), 4 days old *C113S-KVS-1 neurons* (filled circles, fractional current 0.50 ± 0.04, n = 6 cells) and 12 days old *C113S-KVS-1* neurons (hollow circles, fractional current 0.43 ± 0.04, n = 7 cells).

Data are presented as mean ± standard error of the mean (s.e.m). Statistically significant differences are indicated with * ($0.01 < P < 0.05$) and ** ($P < 0.01$).

Table 1

Electrophysiological properties of native ASER potentials

Genotype		V_{12} (mV)	t_{r12} (s)	n
N2	Day 4	55 ± 5.5	0.33 ± 0.03	8
	Day 12	17 ± 2.0 *	0.08 ± 0.01 **	7
	H_2O_2	14 ± 1.0 **	0.09 ± 0.01 **	5
C113S	Day 4	55 ± 6.6	0.30 ± 0.4	6
	Day 12	60 ± 6.0	0.35 ± 0.4	7
	H_2O_2	57 ± 6.1	0.28 ± 0.3	5
tm2034	Day 4	59 ± 5.8	0.08 ± 0.01 **	5
	Day 12	57 ± 6.3	0.07 ± 0.01*	4

V_{12} and t_{r12} indicate the steady-state potential and the time necessary to reach 90 % of steady-state value attained by the cell in response to a current injection of 12 pA. Data are presented as mean ± standard error of the mean (s.e.m). Statistically significant differences are indicated with * (0.01<P<0.05) and ** (P<0.01).